Time optimal and PID controller for armed manipulator robots

FARIDEH GIV, ALAEDDIN MALEK
Department of Applied Mathematics, Faculty of Mathematical Sciences
Tarbiat Modares University
Tehran
IRAN

Abstract: This paper is fourfold. First, three different time-optimal control problems for simulating the manipulator robots with one, two, and three arms are mathematically formulated. Corresponding to the related dynamical systems, the nonlinear system of ordinary differential equations is derived. It has been found that these problems are time-free and have distinct initial and boundary conditions, making them hard to solve. To find the minimum time with different payloads, a successful numerical method based on the finite difference and the three-stage Lobatto formula is proposed. Secondly, the related torque-controlling problems are simulated, and then for one, two, and three armed manipulator robots, they are solved using the PID controller method. Thirdly, it is shown that, compared to the time-optimal controlling problem, the optimal PID torque controller solution takes more time to do the job than was expected. However, the solution in the PID controller method shows less oscillation than the time-optimal control problem. Fourthly, mathematical theories are used, and the numerical results for both methods and different payloads are compared.

Key-Words: armed robot dynamics, time optimal control, proportional-integral-derivative (PID) controller

Received: May 15, 2023. Revised: April 17, 2024. Accepted: May 15, 2024. Published: June 26, 2024.

1 Introduction

The robot is an automatic device that performs functions ordinarily ascribed to human beings, [1], [2].A two-jointed arm light robot without payload (RR-type robot) is introduced by [3]. Robots for manipulating with several rigid links that are controlled by a computer are used to produce things such as electronics, medical devices, optics, and watches, [4]. Most industries today can improve time and facility energy efficiency with light-armed robots, reducing operating costs. Smaller, lighter parts take less time and energy to accelerate, enabling these machines to work faster than their competitors. This speed is ideal for picking, placing, part assembly, sorting, and carrying light payloads. This kind of robot is lighter, so it has less inertia when moving. Their lower weight also means that if a collision occurs, it won't be as damaging, [5].

Since manipulators are typically used to repeat a prescribed task a large number of times, even small improvements in their performances may result in large monetary savings. Here, an attempt is made to reduce the movement time (time optimal control strategy) between two points. Any trajectory that can be realized by applying the available driving forces and connecting the starting point with the target point can be used to implement the maneuver, [6], [7]. Among the optimal control methods, the application of Pontryagin's maximum principle is certainly one of the most widely used. It provides an optimal condition that must be met at each time during the trajectory. The method generally involves restrictions in the form of ordinary differential equations (ODE), which are usually of the first order, therefore limiting the computational cost of their solution up to a certain extent, [8], [9], [10], [11], [12], [13]. One of the most common control algorithms used in the industry is the proportional-integral-derivative (PID) controller (smooth payload transportation strategy), partly because of its robust performance over a wide range of operating conditions as well as its simplicity of operation, [14], [15], [16].

The paper is organized as follows: In Section Armed robot dynamic systems, dynamic systems of armed robots is proposed. The statement of the time optimal control is proposed for armed robots in Section Time optimal control problem . In Section PID controller problem , the problem is described with the PID controller. Numerical

simulation and the corresponding results are given in Section Work Examples. Comprising the results of time optimal control and PID controller discuss in Section Numerical results and discussions and final result is in Section Conclusions.

2 Armed robot dynamic systems

In the year 2020 the behavior of armed robot dynamical systems by using Euler-Lagrange equations are described, [2]:

$$\mathbf{D}(\boldsymbol{\theta}(t))\ddot{\boldsymbol{\theta}}(t)+\mathbf{C}(\boldsymbol{\theta}(t),\dot{\boldsymbol{\theta}}(t))+\mathbf{g}(\boldsymbol{\theta}(t))=\boldsymbol{\tau}(t), \quad (1)$$

where $\boldsymbol{\tau}$ is the generalized force associated with angle $\boldsymbol{\theta}$ (rad). The variable $\boldsymbol{\theta}$ is stated as generalized coordinates θ_1 for a robot with one arm, (θ_1,θ_2) for a robot with two arms and $(\theta_1,\theta_2,\theta_3)$ for a robot with three arms. $\mathbf{D}(\boldsymbol{\theta})$ is the inertia matrix that is symmetric and positive definite in the form, [2].

$$\mathbf{D}(\boldsymbol{\theta})=\sum_{i=1}^{n}(m_i J_{\nu_i}(\theta)^T J_{\nu_i}(\theta) + J_{\omega_i}(\theta)^T R_i(\theta) I_i R_i(\theta)^T J_{\omega_i}(\theta)) , \quad (2)$$

inwhich m_i is the mass of the i-th arm, J_{ν_i} and J_{ω_i} are Jacobian matrices, R_i is the orientation transformation between the body attached frame and the inertial frame, and I_i is the i-th inertial torque. $\mathbf{C}(\boldsymbol{\theta},\dot{\boldsymbol{\theta}})$ is the Christopher matrix

$$c_{kj}=\sum_{i=1}^{n}c_{ijk}(\theta)\dot{\theta}_i=\sum_{i=1}^{n}\frac{1}{2}\left\{\frac{\partial d_{kj}}{\partial\theta_i}+\frac{\partial d_{ki}}{\partial\theta_j}-\frac{\partial d_{ij}}{\partial\theta_k}\right\}\dot{\theta}_i \quad (3)$$

inwhich d_{ij} are components of $\mathbf{D}(\boldsymbol{\theta})$ and $\mathbf{g}(\boldsymbol{\theta})$ is the gravity vector

$$\mathbf{g}(\boldsymbol{\theta})=[g_1(\theta),...,g_n(\theta)]^T , \quad g_k=\frac{\partial P}{\partial\theta_k} . \quad (4)$$

inwhich P is a potential energy. For R-type armed robots $n=1$, $n=2$ for RR-type armed robots and $n=3$ for RRR-type armed robots. The dynamical system (1) consists of a typical second-order nonlinear differential equation (the number of equations corresponds to the number of arms).

The physical characteristics of an armed robot without payload for a robot with two arms are given by [3]. Here, we assume that for R, RR and RRR type robots, L_i is the length for the i-th arm and l_{ci} is the i-th center of mass for $i=1,2,3$ (see Table 1).

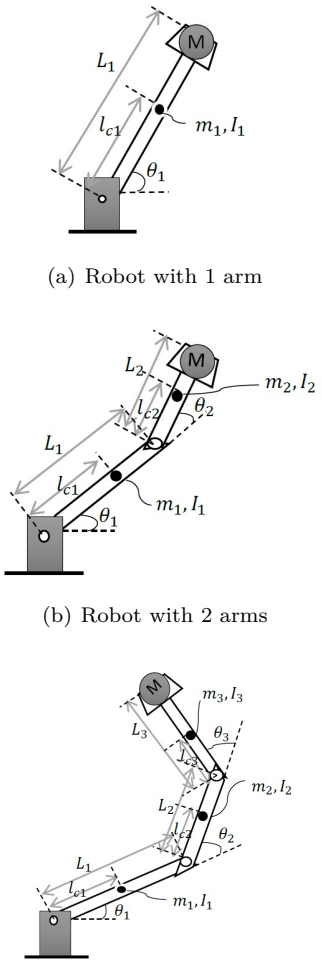

(a) Robot with 1 arm

(b) Robot with 2 arms

(c) Robot with 3 arms

Figure 1: Manipulator robot with payload M, (a) R-type armed (b) RR-type armed, (c) RRR-type armed.

Table 1: Physical characteristics of an armed robot without payload.

Arms # i	L_i (m)	l_{ci} (m)	m_i (kg)	I_i $(kg.m^2)$
1	0.250	0.198	0.193	1.15×10^{-3}
2	0.234	0.143	0.115	4.99×10^{-4}
3	0.218	0.109	0.100	6.58×10^{-4}

According to (1) the dynamic equation for one armed robot (see Figure 1(a)) is

$$\tau_1 = (m_1 l_{c1}^2 + I_1)\ddot{\theta}_1 + m_1 g l_{c1} \cos(\theta_1) \qquad (5)$$

inwhich τ_1 is the corresponding torque for one armed robot. The dynamical system for an RR-type robot in matrix form is as follows (see Figure 1(b) and [2], [17], [18])

$$\begin{pmatrix} \tau_1 \\ \tau_2 \end{pmatrix} = \begin{pmatrix} d_{11} & d_{12} \\ d_{21} & d_{22} \end{pmatrix} \begin{pmatrix} \ddot{\theta}_1 \\ \ddot{\theta}_2 \end{pmatrix} + \begin{pmatrix} h\dot{\theta}_2 & h\dot{\theta}_1 + h\dot{\theta}_2 \\ -h\dot{\theta}_1 & 0 \end{pmatrix} \begin{pmatrix} \dot{\theta}_1 \\ \dot{\theta}_2 \end{pmatrix} + \begin{pmatrix} g_1 \\ g_2 \end{pmatrix} \qquad (6)$$

where

$$\begin{aligned}
d_{11} &= m_1\ l_{c1}^2 + m_2\ (L_1^2 + l_{c2}^2 + 2\ L_1\ l_{c1}^2 \\
&\quad + 2\ L_1\ l_{c2}\ \cos(\theta_2)) + I_1 + I_2, \\
d_{12} &= d_{21} = m_2\ (l_{c2}^2 + L_1\ l_{c2}\ \cos(\theta_2)) + I_2, \\
d_{22} &= m_2\ l_{c2}^2 + I_2, \\
c_{121} &= c_{211} = \tfrac{1}{2}\ \left(\tfrac{\delta d_{11}}{\delta \theta_2}\right) = -m_2\ L_1\ l_{c2} \sin(\theta_2) = h, \\
c_{221} &= \left(\tfrac{\delta d_{12}}{\delta \theta_2}\right) - \tfrac{1}{2}\ \left(\tfrac{\delta d_{22}}{\delta \theta_1}\right) = h, \\
c_{112} &= \left(\tfrac{\delta d_{21}}{\delta \theta_1}\right) - \tfrac{1}{2}\ \left(\tfrac{\delta d_{11}}{\delta \theta_2}\right) = -h, \\
g_1 &= (m_1\ l_{c1} + m_2\ L_1)\ g\ \cos(\theta_1) + m_2\ g\ l_{c2}\ \cos(\theta_1 + \theta_2), \\
g_2 &= m_2\ g\ l_{c2}\ \cos(\theta_1 + \theta_2).
\end{aligned}$$

The dynamical system for RRR-type robot in matrix form is as follows (see Figure 1(c), [14])

$$\begin{pmatrix} \tau_1 \\ \tau_2 \\ \tau_3 \end{pmatrix} = \begin{pmatrix} d_{11} & d_{12} & d_{13} \\ d_{21} & d_{22} & d_{23} \\ d_{31} & d_{32} & d_{33} \end{pmatrix} \begin{pmatrix} \ddot{\theta}_1 \\ \ddot{\theta}_2 \\ \ddot{\theta}_3 \end{pmatrix} + \begin{pmatrix} c_{11} & c_{12} & c_{13} \\ c_{21} & c_{22} & c_{23} \\ c_{31} & c_{32} & c_{33} \end{pmatrix} \begin{pmatrix} \dot{\theta}_1 \\ \dot{\theta}_2 \\ \dot{\theta}_3 \end{pmatrix} + \begin{pmatrix} g_1 \\ g_2 \\ g_3 \end{pmatrix}. \qquad (7)$$

where

$$\begin{aligned}
d_{11} &= I_1 + I_2 + I_3 + \tfrac{1}{4}\ m_1\ L_1^2 + m_2\ (l_{c1}^2 + \tfrac{1}{4}\ L_2^2 \\
&\quad + L_1\ L_2\ \cos(\theta_2)) + m_3\ (L_1^2 + L_2^2 + \tfrac{1}{4}\ L_3^2 + 2\ L_1 \\
&\quad L_3\ \cos(\theta_2) + L_1\ L_3\ \cos(\theta_2 + \theta_3) + L_1\ L_3\ \cos(\theta_3)), \\
d_{12} &= I_2 + I_3 + \tfrac{1}{2}\ m_2\ (\tfrac{1}{2}\ l_{c2}^2 + L_1\ L_2\ \cos(\theta_2)) + m_3 \\
&\quad (2\ L_2^2 + \tfrac{1}{2}\ L_3^2 + 2\ L_1\ L_2 \cos(\theta_2) + L_1\ L_3 \\
&\quad \cos(\theta_2 + \theta_3) + 2\ L_2\ L_3\ \cos(\theta_3)), \\
d_{13} &= I_3 + \tfrac{1}{2}\ (\tfrac{1}{2}\ L_3^2 + L_1\ L_3\ \cos(\theta_2 + \theta_3) + L_2\ L_3 \\
&\quad \cos(\theta_3)), \\
d_{21} &= d_{31} = d_{32} = 0, \\
d_{22} &= I_2 + I_3 + \tfrac{1}{4}\ m_2\ L_2^2 + m_3\ (L_2^2 + \tfrac{1}{4}\ L_3^2 + L_2\ L_3 \\
&\quad \cos(\theta_3)), \\
d_{23} &= I_3 + \tfrac{1}{2}\ m_3\ (L_3^2 + L_2\ L_3\ \cos(\theta_3)), \\
d_{33} &= I_3 + \tfrac{1}{4}\ m_3\ L_3^2,
\end{aligned}$$

$$\begin{aligned}
c_{11} &= c_{21} = c_{31} = 0, \\
c_{12} &= -\tfrac{1}{2}\ m_2\ L_1\ L_2\ \sin(\theta_2)[\dot{\theta}_1 + \dot{\theta}_2 + \tfrac{1}{2}\ \dot{\theta}_3] - m_3\ L_1 \\
&\quad \sin(\theta_2)\ [L_3\ \dot{\theta}_1 + L_2\ (2\ \dot{\theta}_2 + \dot{\theta}_3)] - m_3\ L_1\ L_3 \\
&\quad \sin(\theta_2 + \theta_3)[\tfrac{1}{2}\ \dot{\theta}_1 + \dot{\theta}_2 + \tfrac{1}{2}\ \dot{\theta}_3] - \tfrac{1}{4}\ L_1\ L_3 \\
&\quad \sin(\theta_2 + \theta_3)\ \dot{\theta}_3, \\
c_{13} &= L_3\ \sin(\theta_3)[-\tfrac{1}{2}\ L_2\ (\tfrac{1}{2}\ \dot{\theta}_2 + \dot{\theta}_3) - \tfrac{1}{2}\ m_3\ L_1\ \dot{\theta}_1 \\
&\quad -\tfrac{3}{4}\ m_3\ L_2\ \dot{\theta}_2], \\
c_{22} &= c_{32} = \tfrac{1}{2}\ \dot{\theta}_1\ [L_1\ L_2\ \sin(\theta_2)(\tfrac{1}{2}\ m_2 + 2\ m_3) \\
&\quad +m_3\ L_1\ L_3\ \sin(\theta_2 + \theta_3)], \\
c_{23} &= L_2\ L_3\ \sin(\theta_3)[-\tfrac{1}{2}\ m_3\ (\tfrac{1}{2}\ \dot{\theta}_1 + \dot{\theta}_2 + \dot{\theta}_3) + \tfrac{1}{4}\ \dot{\theta}_1], \\
c_{33} &= \tfrac{1}{4}\ L_2\ L_3\ \sin(\theta_3)[\dot{\theta}_1 - m_3\ \dot{\theta}_2],
\end{aligned}$$

$$\begin{aligned}
g_1 &= \tfrac{1}{2}\ m_1\ g\ L_1 \cos(\theta_1) + m_2\ g\ (L_1 \cos(\theta_1) + \tfrac{1}{2}\ L_2 \\
&\quad \cos(\theta_1 + \theta_2)) + m_3\ g\ (L_1 \cos(\theta_1) + L_2\ \cos(\theta_1 \\
&\quad +\theta_2) + \tfrac{1}{2}\ L_2\ \cos(\theta_1 + \theta_2 + \theta_3)), \\
g_2 &= \tfrac{1}{2}\ m_2\ g\ L_2 \cos(\theta_1 + \theta_2) + m_3\ g\ (L_2\ \cos(\theta_1 \\
&\quad +\theta_2) + \tfrac{1}{2}\ L_3\ \cos(\theta_1 + \theta_2 + \theta_3)), \\
g_3 &= \tfrac{1}{2}\ m_3\ g\ L_3\ \cos(\theta_1 + \theta_2 + \theta_3).
\end{aligned}$$

Now, additional payloads M (see Table 2) will be added to the last arm to make a sensitivity

analysis for the additional payloads with different masses. Note that if one changes the load m_i into $m_i + M$, L_i stays fixed, I_i and l_{ci} will change correspondingly.

Table 2: Masses M that added to the last arm in grams (g).

M (g)	21.2	31.2	51.8	100.6	121.9	130.7	150.5	200	500	1000

3 Time optimal control problem

The aim of designing time optimal control problem here is to consider how one transfer the end-effector of an armed manipulator robot from an initial position to the fixed destination in the minimum possible time and optimal effort. The time optimal control problem is represented by the following performance index:

$$J(u) = \int_{t_0}^{t_f} dt = t_f - t_0, \tag{8}$$

where the final time t_f is unknown, [2], [19], subject to the following nonlinear first order dynamic constraint:

$$\begin{cases} \dot{\mathbf{x}}(t) = \mathbf{f}(\mathbf{x}(t), \boldsymbol{\tau}(t)) \\ \mathbf{x_0} = (\boldsymbol{\theta_0}, \dot{\boldsymbol{\theta}}_\mathbf{0})^T \\ \mathbf{x_{t_f}} = (\boldsymbol{\theta}_{\mathbf{t_f}}, \dot{\boldsymbol{\theta}}_{\mathbf{t_f}})^T \end{cases} \tag{9}$$

inwhich $\mathbf{x}(t) = (\mathbf{x_1}(t), \mathbf{x_2}(t))^T = (\boldsymbol{\theta}(t), \dot{\boldsymbol{\theta}}(t))^T$, that is derived from (5) and (6), for certain initial $\mathbf{x_0} = (\boldsymbol{\theta_0}, \dot{\boldsymbol{\theta}}_\mathbf{0})^T$ and final desired $\mathbf{x_{t_f}} = (\boldsymbol{\theta}_{\mathbf{t_f}}, \dot{\boldsymbol{\theta}}_{\mathbf{t_f}})^T$ conditions, [14]. The minimum time t_f^* denotes the first time that $\mathbf{x}$ posits in the above final desired condition. Note that $\boldsymbol{\theta}$ is *radian* and $\dot{\boldsymbol{\theta}}$ is $\frac{radian}{second}$. Here, for a robot with one arm the vector points $\mathbf{x_0}, \mathbf{x_{t_f}}$ belong to $\mathbf{R}^2$. The function $\mathbf{f}$ depends upon the control parameter $\boldsymbol{\tau}$ is belonging to a set $A \subset \mathbf{R}$, so that $\mathbf{f} : \mathbf{R}^2 \times A \to \mathbf{R}^2$, $\mathbf{x} : [-\pi, \pi] \to \mathbf{R}^2$ and function $\boldsymbol{\tau} : [-3, 3] \to A$ are given. If the robot has two arms $\mathbf{R}^2$ converts to $\mathbf{R}^4$ and if the robot has three arms $\mathbf{R}^2$ converts to $\mathbf{R}^6$.

By applying the Routh-Hurwitz criteria to analyze different stability zones, the stability of the dynamical system is investigated. As well as the modulation equations and detuning parameters, the obtained results offer insights into stable or unstable fixed points, which are illustrated by time history graphs of solutions, phases, and amplitudes.

In the following, we propose two different approaches to solve the optimal control problem (8) and (9). We call this problem as time optimal control problem with the corresponding dynamical system for certain initial $\mathbf{x_0} = (\boldsymbol{\theta_0}, \dot{\boldsymbol{\theta}}_\mathbf{0})^T$ and final desired $\mathbf{x_{t_f}} = (\boldsymbol{\theta}_{\mathbf{t_f}}, \dot{\boldsymbol{\theta}}_{\mathbf{t_f}})^T$ conditions.

The first approach: Although, one can consider the simple dynamics of a vibrating spring where the control is interpreted as an exterior force acting on an oscillating weight of unit mass hanging from a spring, here we use this idea for controlling the armed manipulator robots. For one armed manipulator robot, according to (5) one can write

$$\ddot{\theta_1} = \left(\frac{-m_1 g l_{c1}}{m_1 l_{c1}^2 + I_1}\right) \cos(\theta_1) + \hat{\tau}_1,$$

inwhich $\hat{\tau}_1 = \left(\frac{1}{m_1 l_{c1}^2 + I_1}\right) \tau_1$. The dynamical system is

$$\begin{aligned} \dot{\mathbf{x}}(t) &= \begin{pmatrix} x_2 \\ \left(\frac{-m_1 g l_{c1}}{m_1 l_{c1}^2 + I_1}\right) \cos(x_1) + \hat{\tau}_1 \end{pmatrix} \\ &= \begin{pmatrix} x_2 \\ \left(\frac{-m_1 g l_{c1}}{m_1 l_{c1}^2 + I_1}\right) \cos(x_1) \end{pmatrix} + \begin{pmatrix} 0 \\ \hat{\tau}_1 \end{pmatrix}. \end{aligned} \tag{10}$$

We use the first two terms of the Taylor expansion around point $-\frac{\pi}{2}$ for $\cos(x_1)$ thus

$$\dot{\mathbf{x}}(t) = \begin{pmatrix} x_2 \\ r\,(x_1 + \frac{\pi}{2}) \end{pmatrix} + \begin{pmatrix} 0 \\ k\ \tau_1 \end{pmatrix}, \tag{11}$$

inwhich $r = \frac{-m_1 g l_{c1}}{m_1 l_{c1}^2 + I_1}$ and $k = \frac{1}{m_1 l_{c1}^2 + I_1}$. According to Pontryagin minimum principle, there exists a nonzero vector h such that

$$(h^T \mathbf{x}^{-1}(t) N) \tau_1^*(t) = \max_{\tau_1(.)} \Big\{ (h^T \mathbf{x}^{-1}(t) N) \tau_1(t) \Big\}, \tag{12}$$

where $\tau_1^*(t)$ is the optimal torque for one arm robot, for each time $0 \le t \le t_f^*$. Hence

$$\dot{\mathbf{x}}(t) = \begin{pmatrix} 0 & 1 \\ r & 0 \end{pmatrix} \begin{pmatrix} x_1 \\ x_2 \end{pmatrix} + \begin{pmatrix} 0 \\ k \end{pmatrix} \tau_1 + \begin{pmatrix} 0 & 0 \\ r\frac{\pi}{2} & 0 \end{pmatrix}. \tag{13}$$

Naming

$$\mathbf{M} = \begin{pmatrix} 0 & 1 \\ r & 0 \end{pmatrix}, \ \mathbf{N} = \begin{pmatrix} 0 \\ k \end{pmatrix},$$

yields

$$\mathbf{M}^n = \begin{cases} r^{\frac{n-1}{2}}\mathbf{M} & n = 1, 3, 5, ... \\ r^{\frac{n}{2}}\ I & n = 2, 4, 6, ... \ . \end{cases}$$

In order to derive $\mathbf{x}^{-1}(t)$ in (12) we use the expansion of e^{tM} as

$$\begin{aligned} e^{tM} &= I + tM + \frac{t^2}{2!}M^2 + \frac{t^3}{3!}M^3 + ... \\ &\vdots \\ &= \begin{pmatrix} \cos(rt) & \sin(rt) \\ r\sin(rt) & \cos(rt) \end{pmatrix} \end{aligned}$$

consequently

$$\begin{aligned} \mathbf{x}^{-1}(t) &= \begin{pmatrix} \cos(rt) & \sin(rt) \\ r\sin(rt) & \cos(rt) \end{pmatrix}^{-1} \\ &= \frac{1}{det}\begin{pmatrix} \cos(rt) & -\sin(rt) \\ -r\sin(rt) & \cos(rt) \end{pmatrix} \end{aligned}$$

inwhich $det = \cos^2(rt) - r\sin^2(rt)$. Finally, according to (12) we have

$$\tau_1^*(t) = \frac{k}{det}\ sgn\left(-h_1\sin(rt) + h_2\cos(rt)\right). \quad (14)$$

To simplify further, we choose δ such that

$$h_1 = -\cos(\delta) \quad and \quad h_2 = \sin(\delta)$$

when ${h_1}^2 + {h_2}^2 = 1$. By recalling the trigonometry identity $\sin(a+b) = \sin(a)\cos(b) + \sin(b)\cos(a)$, one can write

$$\tau_1^*(t) = \frac{k}{det}\ sgn\left(\sin(\delta + rt)\right), \quad (15)$$

ie., the optimal control torque is found and τ_1^* switches from $\frac{k}{det}$ to $-\frac{k}{det}$ and vice versa, every $\frac{2\pi}{r}$ units of time. Thus, our goal, which is to design an optimal exterior torque $\tau_1^*(.)$ that brings the motion to a stop in minimum time t_f^* is successfully achieved. Numerical results for a robot with one arm is given in Table 3.

The second approach, [20]: The authors considered the Variation Evolving Method (VEM) that was developed for the classic time-optimal control problem by initializing the transformed IVP with arbitrary initial values of variables. Here, we use their idea to solve the problem of controlling armed manipulator robots in the shortest amount of the shortest amount of time. Mathematically, the difference is that we face initial-boundary-value (IBVP) problems instead of IVP problems. Moreover, we use the first optimize, then discretize technique for a finite-dimensional IBVP as follows:

Table 3: First approach for a robot with one arm.

M (g)	$\frac{2\pi}{r}$	$\pm\frac{k}{det}$
21.2	0.166	2.662
31.2	0.177	2.653
51.8	0.198	2.625
100.6	0.237	2.552
121.9	0.258	2.491
130.7	0.267	2.459
150.5	0.290	2.367
200	0.324	2.232
500	0.452	1.614
1000	0.627	0.354

To solve the time optimal control problems (8) and (9) the Hamiltonian equation

$$H = 1 + \boldsymbol{\rho}^T\dot{\mathbf{x}} \quad (16)$$

is used and for $0 \leq t \leq {t_f}^*$ the response $(\mathbf{x}^*, \boldsymbol{\tau}^*, \boldsymbol{\rho}^*, {t_f}^*)$ according to

$$H(\mathbf{x}^*(t), \boldsymbol{\tau}^*(t), \boldsymbol{\rho}^*(t)) = \min_{\tau} H(\mathbf{x}^*(t), \boldsymbol{\tau}(t), \boldsymbol{\rho}^*(t)), \quad (17)$$

can be computed by solving the following canonical system of equations (optimality conditions)

$$\begin{cases} \dfrac{\partial H}{\partial \mathbf{x}}(\mathbf{x}^*(t), \boldsymbol{\tau}^*(t), \boldsymbol{\rho}^*(t)) = -\dot{\boldsymbol{\rho}}^*(t) \\ \dfrac{\partial H}{\partial \boldsymbol{\rho}}(\mathbf{x}^*(t), \boldsymbol{\tau}^*(t), \boldsymbol{\rho}^*(t)) = \dot{\mathbf{x}}^*(t) \\ H(\mathbf{x}^*(t), \boldsymbol{\tau}^*(t), \boldsymbol{\rho}^*(t))|_{t=t_f^*} = 0, \end{cases} \quad (18)$$

where $\boldsymbol{\tau}^*$ and $\mathbf{x}^*$ are optimal torque and optimal state, $\boldsymbol{\tau}$ and $\mathbf{x}$ are admissible torque and state, $\boldsymbol{\rho}$ is Lagrange multiplier and $\boldsymbol{\rho}^*$ is optimal costate.

For a robot with one arm the Hamiltonian equation is:

$$H = 1 + \rho_1 x_2 + \rho_2 r\cos(x_1) + \rho_2 k\tau.$$

According to (17) one can write

$$\tau_1^* = -\rho_2. \quad (19)$$

For a robot with two arms the Hamiltonian equation is:

$$\begin{aligned} H &= \rho_2(\bar{d_{11}}(\tau_1 - c_1 - g_1) + \bar{d_{12}}(\tau_2 - c_2 - g_2)) \\ &+\rho_4(\bar{d_{21}}(\tau_1 - c_1 - g_1) + \bar{d_{22}}(\tau_2 - c_2 - g_2)) \\ &+\rho_1 x_2 + \rho_3 x_4 + 1, \end{aligned}$$

then from (17) we get

$$\begin{cases} \tau_1^* = -(\rho_2 \bar{d_{11}} + \rho_4 \bar{d_{21}}) \\ \tau_2^* = -(\rho_2 \bar{d_{12}} + \rho_4 \bar{d_{22}}). \end{cases} \tag{20}$$

For a robot with three arms the Hamiltonian equation is:

$$\begin{aligned} H &= \rho_2(\bar{d_{11}}(\tau_1 - c_1 - g_1) + \bar{d_{12}}(\tau_2 - c_2 - g_2) \\ &+\bar{d_{13}}(\tau_3 - c_3 - g_3)) + \rho_4(\bar{d_{21}}(\tau_1 - c_1 - g_1) \\ &+\bar{d_{22}}(\tau_2 - c_2 - g_2) + \bar{d_{23}}(\tau_3 - c_3 - g_3)) \\ &+\rho_6(\bar{d_{31}}(\tau_1 - c_1 - g_1) + \bar{d_{32}}(\tau_2 - c_2 - g_2) \\ &+\bar{d_{33}}(\tau_3 - c_3 - g_3)) + \rho_1 x_2 + \rho_3 x_4 + \rho_5 x_6 + 1, \end{aligned}$$

according to (17) we have

$$\begin{cases} \tau_1^* = -(\rho_2 \bar{d_{11}} + \rho_4 \bar{d_{21}} + \rho_6 \bar{d_{31}}) \\ \tau_2^* = -(\rho_2 \bar{d_{12}} + \rho_4 \bar{d_{22}} + \rho_6 \bar{d_{32}}) \\ \tau_3^* = -(\rho_2 \bar{d_{13}} + \rho_4 \bar{d_{23}} + \rho_6 \bar{d_{33}}) \end{cases} \tag{21}$$

where $\bar{d_{ij}}$ for $i, j = 1, 2, 3$ are components of $\mathbf{D^{-1}}(\boldsymbol{\theta})$. Thus, the response $(\mathbf{x}^*, \boldsymbol{\tau}^*, \boldsymbol{\rho}^*, {t_f}^*)$ can be computed by replacing (19), (20) and (21) into (18) for a robot with one, two and three arms respectively.

4 PID controller problem

In general, the main purpose of a PID controller is to bring the final result of the system process closer to the desired value.

In the year 2015 robust adaptive PID control schemes with known or unknown upper bound of the external disturbances are applied to solve the strong nonlinearity and coupling problems in robot manipulator control problems, [21].

In the year 2016 a PID controller for the simulation of a robotic force control application demonstrating well-damped control with no requirement for a force-rate signal is applied, [22].

In the year 2022 a PID controller for the trajectory tracking of robotic manipulators with known or unknown upper bounds of the uncertainties is applied, [16].

Here, the goal is to carry some payloads from the given starting position to the given final position. Thus, for a defined torque $\hat{\boldsymbol{\tau}}(\boldsymbol{\theta}(t))$ as a controller output, the final form of parallel PID algorithm for an armed manipulator robot is

$$Output(t) \equiv \hat{\boldsymbol{\tau}}(\boldsymbol{\theta}(t)) = \mathbf{D^{-1}}(\boldsymbol{\theta})\ \boldsymbol{\tau}$$

$$= k_P e(\theta(t)) + k_D \frac{de(\theta(t))}{d(t)} + k_I \int_0^t e(\alpha)\, d\alpha \tag{22}$$

where k_P, k_I and k_D are the proportional, integral and derivative gains as tuning parameters, respectively, t is the present time or instantaneous time, α is the variable of integration and $e(\theta(t))$ stands for error. Therefore, the conversion or Laplace transformation function $G(s)$ for the PID controller is

$$G(s) = k_P + \frac{k_I}{s} + k_D\, s, \tag{23}$$

inwhich s is the complex frequency (Laplace transformation variable), [23], [24]. The proportional term involving the k_P coefficient increases system speed and reduces the permanent state differences (but does not take zero). Adding an integral term involving the k_I coefficient vanishes the permanent state differences, but adds a lot of overshoot to the transient response. The derivative term involving k_D coefficient attenuates the transient response fluctuations and brings the step response closer to the ideal desired angle in radians, [18].

Combination of robot dynamic system (1) and PID controller (22) yields

$$\ddot{\boldsymbol{\theta}} = \mathbf{D^{-1}}(\boldsymbol{\theta})[-\mathbf{C}(\boldsymbol{\theta}, \dot{\boldsymbol{\theta}}) - \mathbf{g}(\boldsymbol{\theta})] + \hat{\boldsymbol{\tau}} \tag{24}$$

where the n-vector $\hat{\boldsymbol{\tau}}$ is

$$\hat{\boldsymbol{\tau}} = \mathbf{D^{-1}}(\boldsymbol{\theta})\ \boldsymbol{\tau} \tag{25}$$

and the error or difference is considered as

$$e(\theta_i) = \tilde{\theta_i} - \theta_i\ , \quad i = 1, ..., n \tag{26}$$

inwhich $\tilde{\theta_i}$ is the given final position and θ_i is the instantaneous final position of each joint for the arm robot in radians.

From (22) and (23), the matrix form for the PID controller of each conversion function vector input is

$$\hat{\boldsymbol{\tau}} = \mathbf{k_P}\ \mathbf{e} + \mathbf{k_D}\ \dot{\mathbf{e}} + \mathbf{k_I} \int \mathbf{e}\ dt. \tag{27}$$

According to robot dynamic (24) and PID controller algorithm (27) for one armed robot (R-type) we have

$$\ddot{\theta}_1 = \frac{-m_1 g l_{c1} \cos(\theta_1)}{m_1 l_{c1}^2 + I_1} + k_{P_1}(\tilde{\theta_1} - \theta_1) + k_{D_1}\dot{\theta}_1 + k_{I_1}\int e(\theta_1)\, dt, \tag{28}$$

for two armed robot (RR-type) we get

$$\begin{pmatrix} \ddot{\theta}_1 \\ \ddot{\theta}_2 \end{pmatrix} = \begin{pmatrix} d_{11} & d_{12} \\ d_{21} & d_{22} \end{pmatrix}^{-1} \Big[- \begin{pmatrix} h\ \dot{\theta}_2 & h\ \dot{\theta}_1 + h\ \dot{\theta}_2 \\ -h\ \dot{\theta}_1 & 0 \end{pmatrix} \begin{pmatrix} \dot{\theta}_1 \\ \dot{\theta}_2 \end{pmatrix} - \begin{pmatrix} g_1 \\ g_2 \end{pmatrix} \Big] + \begin{pmatrix} k_{P_1}(\tilde{\theta_1} - \theta_1) + k_{D_1}\dot{\theta}_1 + k_{I_1}\int e(\theta_1)\, dt \\ k_{P_2}(\tilde{\theta_2} - \theta_2) + k_{D_2}\dot{\theta}_2 + k_{I_2}\int e(\theta_2)\, dt \end{pmatrix} \tag{29}$$

and for three armed robot (RRR-type) we can write

$$\begin{pmatrix} \ddot{\theta}_1 \\ \ddot{\theta}_2 \\ \ddot{\theta}_3 \end{pmatrix} = \begin{pmatrix} d_{11} & d_{12} & d_{13} \\ d_{21} & d_{22} & d_{23} \\ d_{31} & d_{32} & d_{33} \end{pmatrix}^{-1} \Big[- \begin{pmatrix} c_{11} & c_{12} & c_{13} \\ c_{21} & c_{22} & c_{23} \\ c_{31} & c_{32} & c_{33} \end{pmatrix} \begin{pmatrix} \dot{\theta}_1 \\ \dot{\theta}_2 \\ \dot{\theta}_3 \end{pmatrix} - \begin{pmatrix} g_1 \\ g_2 \\ g_3 \end{pmatrix} \Big] + \begin{pmatrix} k_{P_1}(\tilde{\theta_1} - \theta_1) + k_{D_1}\dot{\theta}_1 + k_{I_1}\int e(\theta_1)\, dt \\ k_{P_2}(\tilde{\theta_2} - \theta_2) + k_{D_2}\dot{\theta}_2 + k_{I_2}\int e(\theta_2)\, dt \\ k_{P_3}(\tilde{\theta_3} - \theta_3) + k_{D_3}\dot{\theta}_3 + k_{I_3}\int e(\theta_3)\, dt \end{pmatrix}. \tag{30}$$

The problem here is defined as the determination of the best possible control strategy (optimal control torque vector $\hat{\boldsymbol{\tau}}$), which minimizes a performance index as the difference between the given desired position and the instantaneous final position of each joint arm. The last arm has a payload of mass M and the goal is to transport the mass M from the initial position into the desired position. The robot dynamic system under control is described in (28), (29) and (30) for a robot with one, two and three arms respectively. Thus, the general corresponding optimal parallel PID controller problem is as follows:

$$\begin{cases} \min_\tau \ J = \int_{t_0}^{t_f} \ \mathbf{e}(\boldsymbol{\theta}, \dot{\boldsymbol{\theta}})\ dt, \\ \quad S.t. \\ \quad\quad \ddot{\boldsymbol{\theta}} = \mathbf{D^{-1}}(\boldsymbol{\theta})[-\mathbf{C}(\boldsymbol{\theta}, \dot{\boldsymbol{\theta}}) - \mathbf{g}(\boldsymbol{\theta})] \\ \quad\quad\quad + \mathbf{k_P}\ \mathbf{e} + \mathbf{k_D}\ \dot{\mathbf{e}} + \mathbf{k_I}\ \int\ \mathbf{e}\ dt \\ \quad\quad \mathbf{x_0} = (\boldsymbol{\theta_0}, \dot{\boldsymbol{\theta}}_\mathbf{0})^T \\ \quad\quad \mathbf{x_{t_f}} = (\boldsymbol{\theta}_{\mathbf{t_f}}, \dot{\boldsymbol{\theta}}_{\mathbf{t_f}})^T. \end{cases} \tag{31}$$

Note that, this problem is not considered the minimum time control problem since the terminal time is not free. This problem can be called a fixed endpoint for a fixed time to some great enough time extension. Moreover, components of the n-vector $\hat{\boldsymbol{\tau}}$ increase as the robot's arms increase. Thus, we face a nonlinear problem that is far too difficult to solve, since the corresponding dynamical problem is IBVP. To overcome these difficulties, the parallel PID controller technique for manipulator robots with one, two and three arms (R, RR and RRR types) is proposed, [14].

5 Work Examples

For one, two and three armed manipulator robots with the assumptions in Table 1 and Table 2. *Firstly*, we consider three optimal time control problems in Work Examples 1, 2 and 3. The performance index is stated by (8) while in the nonlinear dynamical system, initial and final states are given by (9). *Secondly*, in Work Examples 4, 5 and 6 we consider three parallel PID controller problems as described by (31). In both cases, control is the torque $\boldsymbol{\tau}(t)$ while $\mathbf{x}(t)$ and $\boldsymbol{\rho}(t)$ are state and costate, respectively. *Then*, we compare and discuss the numerical results for all the above cases.

5.1 Example 1 (time optimal for R-type robot)

In this example, the one armed manipulator robot (see Figure 1(a)) for carrying 10 different loads in Table 2 from angle position $\frac{-\pi}{2}$ to angle position $\frac{\pi}{20}$ is considered. The initial and final desired conditions are:

$$\begin{pmatrix} \theta_1(0) \\ \dot{\theta}_1(0) \end{pmatrix} = \begin{pmatrix} \frac{-\pi}{2} \\ 0 \end{pmatrix} and \begin{pmatrix} \theta_1(t_f^*) \\ \dot{\theta}_1(t_f^*) \end{pmatrix} = \begin{pmatrix} \frac{\pi}{20} \\ 0 \end{pmatrix}$$

respectively. The optimal total time t_f^* is unknown and will be found. The optimal angle $\theta^*(t)$, velocity $\dot{\theta}^*(t)$ and torque $\tau^*(t)$ for $t \in [0, t_f^*]$ must be found.

5.2 Example 2 (time optimal for RR-type robot)

Here, the two armed manipulator robot (see Figure 1(b)) for carrying 10 different loads in Table 2 from angle position $(\frac{-\pi}{2}, \frac{\pi}{84})$ to angle position $(\frac{\pi}{20}, \frac{-\pi}{84})$ is considered. The initial and final desired conditions are:

$$\begin{pmatrix} \theta_1(0) \\ \theta_2(0) \\ \dot{\theta}_1(0) \\ \dot{\theta}_2(0) \end{pmatrix} = \begin{pmatrix} \frac{-\pi}{2} \\ \frac{\pi}{84} \\ 0 \\ 0 \end{pmatrix} and \begin{pmatrix} \theta_1(t_f^*) \\ \theta_2(t_f^*) \\ \dot{\theta}_1(t_f^*) \\ \dot{\theta}_2(t_f^*) \end{pmatrix} = \begin{pmatrix} \frac{\pi}{20} \\ \frac{-\pi}{84} \\ 0 \\ 0 \end{pmatrix}$$

respectively. The optimal total time t_f^* is unknown and will be found. The optimal angle $\theta^*(t)$, velocity $\dot{\theta}^*(t)$ and torque $\tau^*(t)$ for $t \in [0, t_f^*]$ must be found.

5.3 Example 3 (time optimal for RRR-type robot)

In this Example the state is $X(t) = (\theta_1(t), \theta_2(t), \theta_3(t), \dot{\theta}_1(t), \dot{\theta}_2(t), \dot{\theta}_3(t))^T$.

The three armed manipulator robot (see Figure 1(c)) for carrying 10 different loads in Table 2 from angle position $(\frac{-\pi}{2}, \frac{\pi}{84}, \frac{-\pi}{84})$ to angle position $(\frac{\pi}{20}, \frac{-\pi}{84}, \frac{\pi}{84})$ is considered. The initial and final desired conditions are:

$$\begin{pmatrix} \theta_1(0) \\ \theta_2(0) \\ \theta_3(0) \\ \dot{\theta}_1(0) \\ \dot{\theta}_2(0) \\ \dot{\theta}_3(0) \end{pmatrix} = \begin{pmatrix} \frac{-\pi}{2} \\ \frac{\pi}{84} \\ \frac{-\pi}{84} \\ 0 \\ 0 \\ 0 \end{pmatrix} and \begin{pmatrix} \theta_1(t_f^*) \\ \theta_2(t_f^*) \\ \theta_3(t_f^*) \\ \dot{\theta}_1(t_f^*) \\ \dot{\theta}_2(t_f^*) \\ \dot{\theta}_3(t_f^*) \end{pmatrix} = \begin{pmatrix} \frac{\pi}{20} \\ \frac{-\pi}{84} \\ \frac{\pi}{84} \\ 0 \\ 0 \\ 0 \end{pmatrix}$$

respectively. The optimal total time t_f^* is unknown and will be found. The optimal angle $\theta^*(t)$, velocity $\dot{\theta}^*(t)$ and torque $\tau^*(t)$ for $t \in [0, t_f^*]$ must be found.

Examples 4, 5 and 6 are about PID control for one-armed two-armed and three-armed robots, respectively. In Section 4, we described the method of calculating PID controller problem is proposed. In Examples 4, 5 and 6, the initial and final position values are fixed while the optimal torque is computed by specifying PID coefficients. The speed and position of the one and two armed robots with the optimal torque are shown in Figure 3, Figure 5 and Figure 7 respectively.

5.4 Example 4 (PID controller for R-type robot)

The one armed manipulator robot for carrying 10 different loads from angle position $\theta_0 = \frac{-\pi}{2}$ to angle position $\theta_{t_f} = \frac{\pi}{20}$, with the initial and final velocity equal to zero $(\dot{\theta}_0 = \dot{\theta}_{t_f} = 0, \frac{rad}{sec})$ is considered. Suppose that $t \in [0, 10]$, i.e., $t_f = 10$ is long enough time to complete the robot work process. The coefficients of the PID controller are:

$$k_{P_1} = 30,\ k_{D_1} = 10,\ k_{I_1} = 50 \tag{32}$$

5.5 Example 5 (PID controller for RR-type robot)

Here, the two armed manipulator robot for carrying 10 different loads from angle position $\boldsymbol{\theta}_0 = (\frac{-\pi}{84}, \frac{\pi}{84})$ to angle position $\boldsymbol{\theta}_{t_f} = (\frac{\pi}{84}, \frac{-\pi}{84})$ and the initial and final velocity equal to zero $(\dot{\boldsymbol{\theta}}_{\mathbf{0}} = \dot{\boldsymbol{\theta}}_{\boldsymbol{t_f}} = 0, \frac{rad}{sec})$ is considered. Suppose that $t \in [0, 10]$, i.e., $t_f = 10$ is long enough time to complete the robot work process. The PID coefficients are:

$$k_{P_i} = 30,\ k_{D_i} = 10,\ k_{I_i} = 50, \quad i = 1, 2 \tag{33}$$

5.6 Example 6 (PID controller for RRR-type robot)

The three armed manipulator robot for carrying 10 different loads from angle position $\boldsymbol{\theta}_0 = (\frac{-\pi}{2}, \frac{\pi}{84}, \frac{-\pi}{84})$ to angle position $\boldsymbol{\theta}_{t_f} = (\frac{\pi}{20}, \frac{-\pi}{84}, \frac{\pi}{84})$, with the initial and final velocity equal to zero $(\dot{\boldsymbol{\theta}}_{\mathbf{0}} = \dot{\boldsymbol{\theta}}_{\boldsymbol{t_f}} = 0, \frac{rad}{sec})$ is considered. Suppose that $t \in [0, 10]$, i.e., $t_f = 10$ is long enough time to complete the robot work process. The PID coefficients are:

$$k_{P_i} = 30,\ k_{D_i} = 10,\ k_{I_i} = 50, \quad i = 1, 2, 3 \tag{34}$$

6 Numerical results and discussions

In this section, we discuss the numerical results calculated for Examples 1, 2, 3, 4, 5 and 6. We remind you that in each of the examples in the Work Example section, 10 different masses in Table 2 are added to the end of the last arm of each of the one, two, and three armed robots. The results related to the total time process are presented in Table 4, Table 5 and Table 6. In these tables, the first column is related to the mass added to the last arm, and the second column is the computed minimum total time of the solution in problems (8) and (9). The third column is related to the solution for the problem (31). Total times in Table 4, Table 5 and Table 6 show the period time when the robot is placed in the given final position for the first time. Examples 1, 2 and 3 are solved. Figure 2, Figure 4 and Figure 6 are optimal position, velocity and torque diagrams obtained from solving the time optimal control problems (8) and (9). Examples 4, 5 and 6 are solved. Figure 3,

Figure 5 and Figure 7 are optimal position, velocity and torque diagrams obtained from solving the PID controller problem (31). Note that all 10 payloads are used. However, the graphs are presented for the mass of 100.6 (g) and for the rest of the masses, only the times are calculated and given in tables.

In Section 6.1, results for Examples 1 and 4 are compared when the one-armed robot is used. Example 1 is the optimal time control problem while Example 4 is a PID controller problem. According to Figure 2 and Figure 3, some resulting data are compared in Table 4. Total time, Oscillations, Range of speeds, Effect of payloads, and Stability are discussed and compared for Examples 1 and 4.

6.1 Results comparison for Example 1 and 4

Numerical results for the solutions in Examples 1 and 4 for manipulator robots with one arm (see Table 4, Figure 2 and Figure 3) show that:
(i) (Total time) Due to Figure 2, the minimum time is $t_f^* = 0.3319$ seconds. In Example 4, for the PID controller problem (see Figure 3), it takes about 4.317 seconds for the payload to be in the given final position for the first time (comparison can be made by considering Table 4, Figure 2 and Figure 3).
(ii) (Oscillations) The range of changes for position, velocity and torque in Example 1 (see Figure 2) are greater than the corresponding results for the PID controller problem (see Figure 3). In an optimal time control problem, one needs that the robot move very quickly to reach the final given position in the posible minimum time. In Example 4, one needs to minimize the states during the total time with the best possible torque. Thus we expect a longer period of time with smoother graphs compared to the resultes in Example 1.
(iii) (Range of speeds) Velocity comparison (see Figure 2(b) and Figure 3(b)) shows that the range of the velocity values in Example 1 is greater than the velocity values in Example 4.
(iv) (Effect of payloads) Both problems for different payloads are solved. As the payloads are increased, the time in both Examples 1 and 4 increases (see Table 4).
(v) (Stability) As it is shown in Figure 3(a), Figure 3(b) and Figure 3(c) the solutions stay stable even after the minimum torque is found. In Example 1, after $t = t_f^*$ the process of computing is stopped.

In the minimum time control problem, one reaches the final destination in the least time, (with almost 3 oscillations in 0.312 to 0.405 sec-

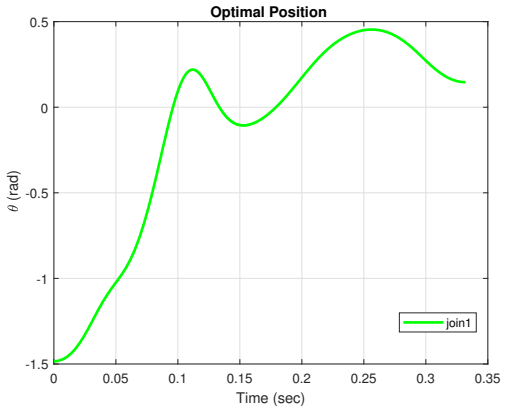

(a) Optimal position value for robot with 1 arm

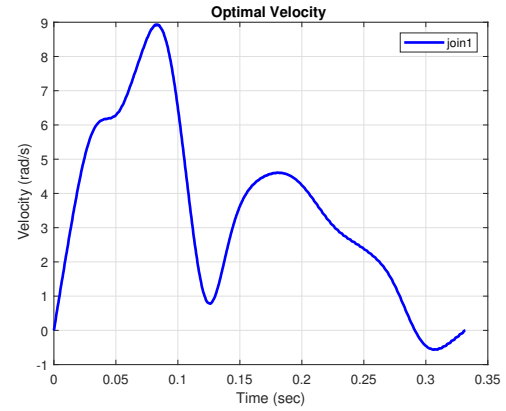

(b) Optimal velocity value for robot with 1 arm

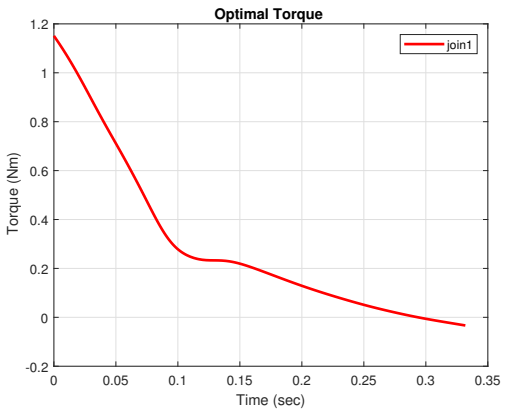

(c) Optimal torque value for robot with 1 arm

Figure 2: (**Example 1**) Time optimal control solutions for an R-type armed manipulator robot with a payload of 100.6 (g). As it is shown in the three different graphs, the optimal minimum time is $t_f^* = 0.3319$ (sec) and it is computed in the process of solving the problem in Example 1: (a) Optimal Position values against time are depicted (b) Optimal Velocity values against time are depicted (c) Optimal Torque values against time are depicted.

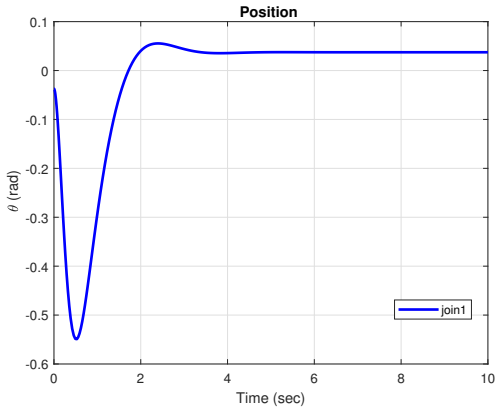

(a) Position value for robot with 1 arm

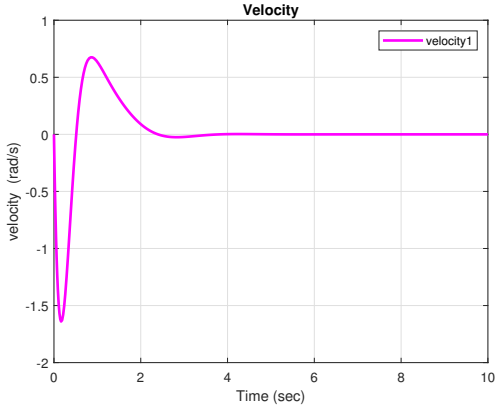

(b) Velocity value for robot with 1 arm

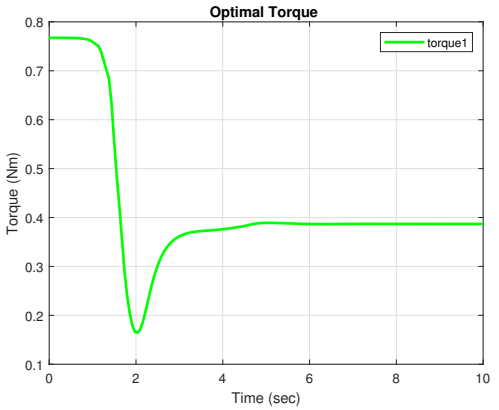

(c) Optimal torque value for robot with 1 arm

Figure 3: (**Example 4**) PID controller numerical solutions for R-type armed manipulator robot with payload 100.6 (g). As it is shown in the three different graphs, the optimal minimum torque is 0.3891 (Nm) at time 4.317 seconds (see Figure 3(c)) and it is computed in the process of solving the problem in Example 4: (a) Position values (corresponding to the optimal torque value) against time are depicted (b) Velocity values (corresponding to the optimal torque value) against time are depicted (c) Optimal Torque values against time are depicted.

Table 4: Total time (sec) for R-type manipulator robot.

M (g)	Total time (Example 1)	Total time (Example 4)
21.2	0.312	4.260
31.2	0.321	4.271
51.8	0.330	4.301
100.6	0.331	4.317
121.9	0.347	4.328
130.7	0.358	4.336
150.5	0.363	4.345
200	0.382	4.369
500	0.395	4.415
1000	0.405	4.502

onds for mass between 21.2 to 1000 grams) however this itself causes wear and tear and sometimes damage to the robot.

6.2 Results comparison for Example 2 and 5

Numerical results for the solutions in Examples 2 and 5 for a manipulator robot with two arms (see Table 5, Figure 4 and Figure 5) show that:
(i) (Total time) Due to Figure 4, the minimum time is $t_f^* = 0.3837$ seconds. In Example 5, for the PID controller problem (see Figure 5), it takes about 4.607 seconds for the payload to be in the given final position for the first time (comparison can be made by considering Table 5, Figure 4 and Figure 5).
(ii) (Oscillations) The corresponding fluctuations of the position, velocity and torque graphs for Example 2 (see Figure 4) are greater than the results of the PID controller problem (see Figure 5). Since, in an optimal time control problem, one needs the robot to move quickly enough to reach the final given position in the minimum time. As it was expected in Example 5, (one needs to do the work with the best torque), thus we expect a longer period of time with smoother graphs compared to the results of Example 2, while the optimal torque value by solving problem (31) is greater (see Figure 4(c) and Figure 5(c)).
(iii) (Range of speeds) Velocity comparison (see Figure 4(b) and Figure 5(b)) shows that the range of the velocity values in Example 2 is greater than the velocity values in Example 5.
(iv) (Effect of payloads) Both problems for different payloads are solved. As the payloads are increased, the time in both Examples 2 and 5 in-

creases (see Table 5).
(v) (Stability) As it is shown in Figure 5(a), Figure 5(b) and Figure 5(c) the solutions stay stable even after the minimum torque is found. In Example 2, after $t = t_f^*$ the process of computing is stopped.

Table 5: Total time (sec) for RR-type manipulator robot.

M (g)	Total time (Example 2)	Total time (Example 5)
21.2	0.342	4.213
31.2	0.360	4.320
51.8	0.379	4.568
100.6	0.383	4.607
121.9	0.399	4.779
130.7	0.410	4.880
150.5	0.432	4.995
200	0.449	5.005
500	0.560	5.012
1000	0.584	5.029

6.3 Results comparison for Example 3 and 6

Numerical results for the solutions in Examples 3 and 6 for a manipulator robot with three arms (see Table 6, Figure 6 and Figure 7) show that:
(i) (Total time) Due to Figure 6, the minimum time is $t_f^* = 0.6257$ seconds. In Example 6, for the PID controller problem (see Figure 6), it takes about 6.235 seconds for the payload to be in the given final position for the first time (comparison can be made by considering Table 6, Figure 6 and Figure 7).
(ii) (Oscillations) The corresponding fluctuations of the position, velocity and torque graphs for Example 3 (see Figure 6) are greater than the results of the PID controller problem (see Figure 7). Since, in an optimal time control problem, one needs that the robot move quickly enough to reach the final given position in the minimum time. As it was expected in Example 6, (one needs to do the work with the best torque), thus we expect a longer period of time with more smooth graphs compared to the results of Example 3, while the optimal torque value by solving problem (31) is greater (see Figure 6(c) and Figure 7(c)).
(iii) (Range of speeds) Velocity comparison (see Figure 6(b) and Figure 7(b)) shows that the range of the velocity values in Example 3 is greater than the velocity values in Example 6.

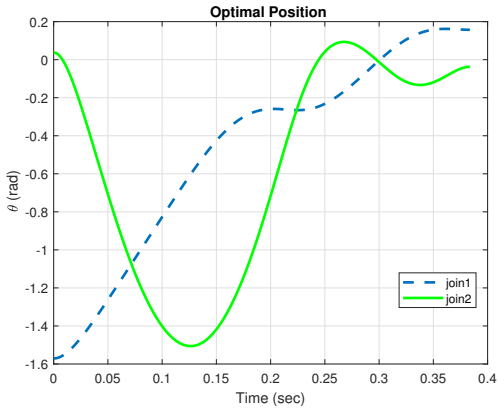

(a) Optimal position value for robot with 2 arms

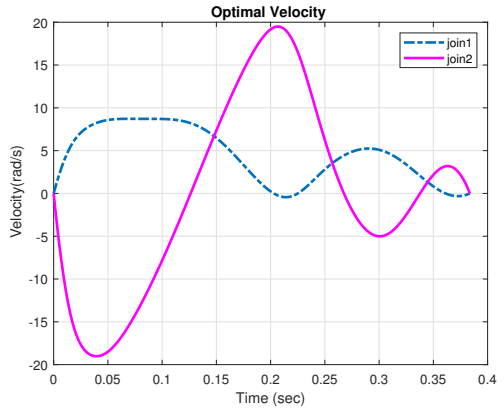

(b) Optimal velocity value for robot with 2 arms

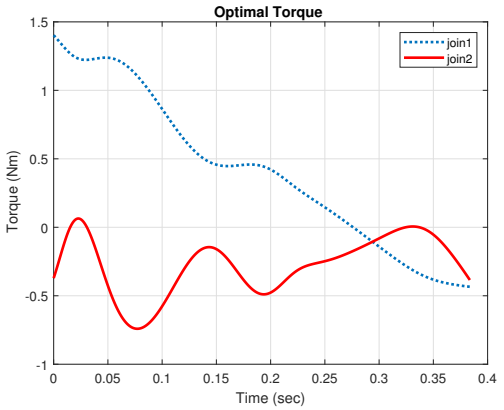

(c) Optimal torque value for robot with 2 arms

Figure 4: (**Example 2**) Time optimal control solutions for an RR-type armed manipulator robot with a payload 100.6 (g). As it is shown in the three different graphs, the optimal minimum time is $t_f^* = 0.3837$ (sec) and it is computed in the process of solving the problem in Example 2: (a) Optimal Position values against time are depicted (b) Optimal Velocity values against time are depicted (c) Optimal Torque values against time are depicted.

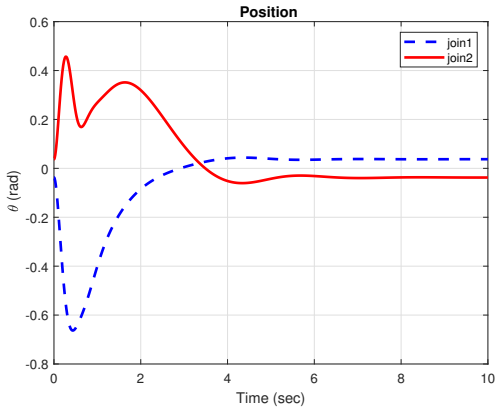

(a) Position value for robot with 2 arms

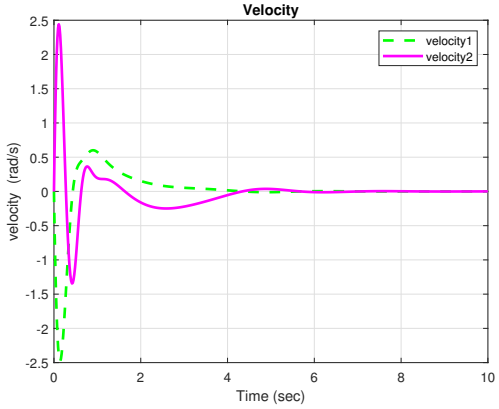

(b) Velocity value for robot with 2 arms

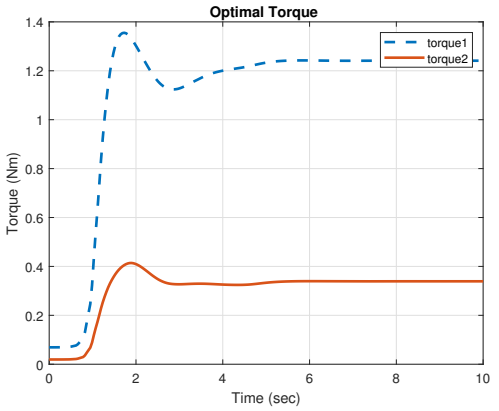

(c) Optimal torque value for robot with 2 arms

Figure 5: (**Example 5**) PID controller numerical solutions for RR-type armed manipulator robot with payload 100.6 (g). As it is shown in the three different graphs, the optimal minimum torque for the first joint 1.242 (Nm) and the second joint 0.3396 (Nm) at time 4.607 seconds is calculated (see Figure 6(c)) and it is computed in the process of solving the problem in Example 5: (a) Position values (corresponding to the optimal torque value) against time are depicted (b) Velocity values (corresponding to the optimal torque value) against time are depicted (c) Optimal Torque values against time are depicted.

(iv) (Effect of payloads) Both problems for different payloads are solved. As the payloads are increased, the time in both Examples 3 and 6 increases (see Table 6).
(v) (Stability) As it is shown in Figure 7(a), Figure 7(b) and Figure 7(c), the solutions stay stable even after the minimum torque is found. In Example 1, after $t = t_f^*$ the process of computing is stopped.

Table 6: Total time (sec) for RRR-type manipulator robot.

M (g)	Total time (Example 3)	Total time (Example 6)
21.2	0.566	6.202
31.2	0.582	6.218
51.8	0.601	6.229
100.6	0.625	6.235
121.9	0.651	6.248
130.7	0.683	6.260
150.5	0.701	6.275
200	0.719	6.298
500	0.723	6.354
1000	0.758	6.407

6.4 Total torques computation for Examples 1 to 6

The trapezoidal numerical integral method is used to calculate the total torque for each arm.

$$\int_{t_0}^{t_f} |\tau_{total}(t)|\, dt = \frac{t_f - t_0}{2N} \sum_{n=1}^{N} [|\tau_{total}(t_n)| + |\tau_{total}(t_{n+1})|] \tag{35}$$

where the spacing between each point is equal to the scalar value $\frac{t_f - t_0}{N} = 1$.

The numerical results for robots of R, RR and RRR types with payload of 100.6 (g) are given in Table 7. According to Table 7, the total torque increases with the increase in the number of arms in Examples 1, 2, ..., 6. In the PID controller strategy for RR and RRR type robots, it is found that the first arm consumes more torque compared to the other arms.

7 Conclusions

This paper presents the mathematical simulation of an armed manipulator robot of R, RR, RRR type for the application of lifting and moving light

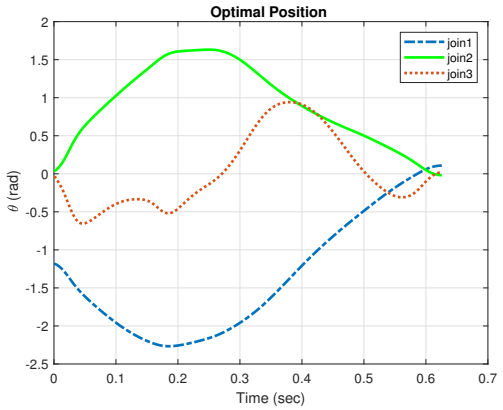

(a) Optimal position value for robot with 3 arms

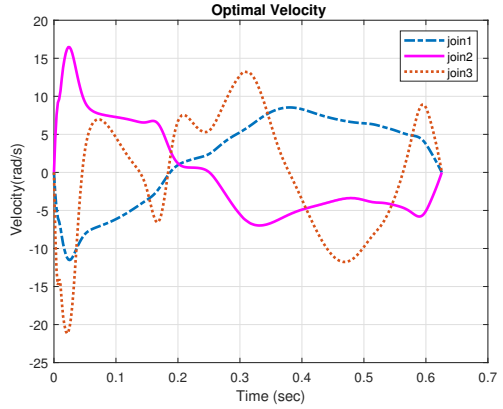

(b) Optimal velocity value for robot with 3 arms

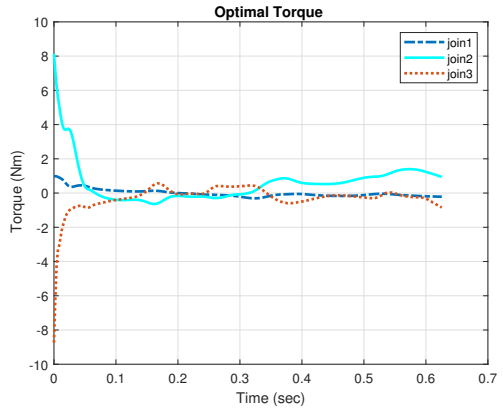

(c) Optimal torque value for robot with 3 arms

Figure 6: (**Example 3**) Time optimal control solutions for an RRR-type armed manipulator robot with a payload of 100.6 (g). As it is shown in the three different graphs, the optimal minimum time is $t_f^* = 0.6257$ (sec) and it is computed in the process of solving the problem in Example 3: (a) Optimal Position values against time are depicted (b) Optimal Velocity values against time are depicted (c) Optimal Torque values against time are depicted.

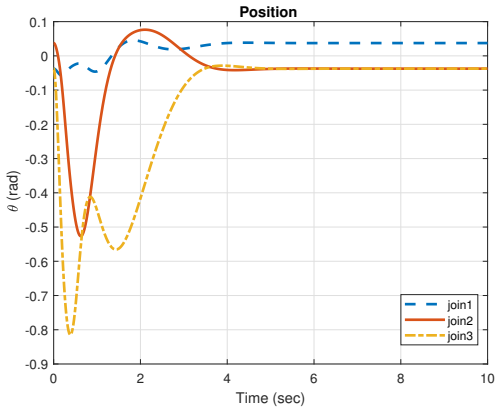

(a) Position value for robot with 3 arms

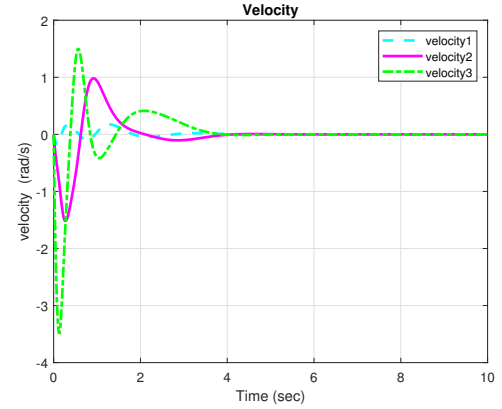

(b) Velocity torque value for robot with 3 arms

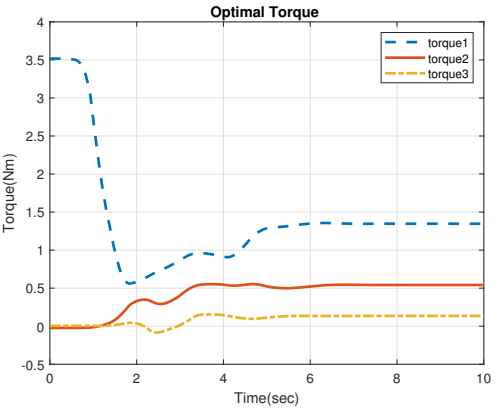

(c) Optimal torque value for robot with 3 arms

Figure 7: (**Example 6**) PID controller numerical solutions for RRR-type armed manipulator robot with payload 100.6 (g). As it is shown in the three different graphs, the optimal minimum torque for the first joint 1.356 (Nm), the second joint 0.5411 (Nm) and the third joint 0.1338 (Nm) at time 6.235 seconds is calculated (see Figure 7(c)) and it is computed in the process of solving the problem in Example 6: (a) Position values (corresponding to the optimal torque value) against time are depicted (b) Velocity values (corresponding to the optimal torque value) against time are depicted (c) Optimal Torque values against time are depicted.

Table 7: Total torque (Nm) for Examples 1 to 6.

Robot type	Example #	Total torque
R-type	1	$\|\tau_1\| = 0.0977$
	4	$\|\tau_1\| = 1.9141$
RR-type	2	$\|\tau_1\| = 0.2171$
		$\|\tau_2\| = 0.1062$
	5	$\|\tau_1\| = 4.7883$
		$\|\tau_2\| = 1.3450$
RRR-type	3	$\|\tau_1\| = 0.1062$
		$\|\tau_2\| = 0.5022$
		$\|\tau_3\| = 0.2673$
	6	$\|\tau_1\| = 8.8336$
		$\|\tau_2\| = 2.5010$
		$\|\tau_3\| = 0.5668$

material objects between 21 to 1000 grams. The torque controller is used to control the servo motor in combined motion and the robot end-effector. The robotic problem is mathematically formulated as: (i) The Time Optimal Control Problem, (ii) The PID Controller Problem. Numerical results show that the first strategy gives better solutions considering time, speed and torque consumption. However, the PID controller strategy will give a smoother solution with relatively greater torque, a lower speed and a longer time. In both cases, manipulator robots can successfully move objects with a maximum weight of 1 kg based on the given robotic assumptions and problem hypotheses. The final conclusion in the application of method 1 and 2 is that although method 1 announces smaller numerical results, in practice it may cause the failure of the devices, while in method 2, although the numerical results are larger, but from the point of view of damage to the devices, it is reasonable It looks better. Moreover, computational results show that when the number of jointed arms is increased both total time and total torque increase, respectively. However, in the PID strategy, when we add an arm to the robot, the operational torque needed for the first arm is greater than the others.

8 Future work

We intend to investigate the following topics in the future:

(i) The use of artificial intelligence as well as interval calculations for the problem of the least optimal time for the robot dynamic system.

(ii) Combination of the methods with Luenberger observers.

(iii) Combinations of the methods with computational Intelligence.

(iv) Stability and the stability margin of the system.

References:

[1] Isabel M, Ferreira A, Sequeira J and Virk G (2020) *Robotics and Well-Being*. Springer.

[2] Spong M, Hutchinson W and Vidyassagar S (2020) *Robot Modeling and Control*. Wilely.

[3] Gallant A and Gosselin C (2018) Extending the capabilities of robotic manipulators using trajectory optimization. *Mechanism and Machine Theory*. 121. 502-514.

[4] Weber A (2020) Small robots play a big tole in automation. *Assembly Magazine*.

[5] Partida D (2021) Benefits of miniature industrial robots. *Robotics Tomorrow*. 21 September 2021.

[6] Malek A, Jafarian-Khaled Abad L and Khodayari-Samghabadi S (2015) Semi-Infinite programming to solve armed robot trajectory problem using recurrent neural network. *International Journal of Robotics and Automation*. 30 (2).

[7] Jazar RN (2022) Time optimal control. In: *Theory of Applied Robotics (pp. 731-757), Springer, Cham*.

[8] Gattringer H, Mueller A, Oberherber M and Kaserer D (2022) Time-optimal robotic manipulation on a predefined path of loosely placed objects. *Modeling and experiment. Mechatronics*. 84, 102753.

[9] Rojas-Quintero JA, Dubois F and Ramirez-de-Avila HC (2022) Riemannian formulation of Pontryagin's maximum principle for the 0ptimal control of robotic manipulators. *Mathematics*. 10(7) 1117.

[10] Troltzsch F (2024) *Optimal Control of Partial Differential Equations Theory, Methods and Applications.*Amer Mathematical Society.

[11] Rojas-Quintero JA, Rojas-Estrada JA, Villalobos-Chin J, Satibanez V and Bugarin E (2022) Optimal controller applied to robotic systems using covariant control equations. *International Journal of Control*. 95(6): 1576-89.

[12] Ferrentino E, Cioppa A D, Marcelli A and Chiacchio P (2020) An Evolutionary Approach to Time-Optimal Control of Robotic Manipulators. *Journal of Intelligent & Robotic Systems*. 99: 245-260.

[13] Jin W, Kulic D, Mou S and Hirche S (2021) Inverse optimal control from incomplete trajectory observations. *The International Journal of Robotics Research*. 40(6-7):848-865.

[14] Giv F and Malek A (2024) Proportional-integral-derivative controller for armed manipulator robots. *International journal of robotics and automation*. 39(3): 170-180.

[15] Sachan S, Goud H and Swarnkar P (2022) Performance and stability analysis of industrial robot manipulator. *In Intelligent Computing Techniques for Smart Energy* . Springer. pp. 473-481.

[16] Qiao L, Zhao M, Wu C, Ge T, Fan R and Zhang W (2022) Adaptive PID control of robotic manipulators without equality/inequality constraints on control gains. *International Journal of Robust and Nonlinear Control*. 32(18): 9742-9760.

[17] Alonso E and Garcia M (2015) *Numerical Modelling in Robotics*. OmniaScience.

[18] Verl A, Schaffer A, Raatz A and Brock O (2015) *Soft Robotics Transferring Theory to Application*. Springer Verlag.

[19] Aschepkov LT, Dolgy DV, Kim T and Agarwal P (2016) *Optimal control*. Springer.

[20] Zhang S and Qian W (2017) Computation of time-optimal control problem with variation evolution principle. *arXiv*. 1711.02998.

[21] Xu J and Qiao L (2015) Robust adaptive PID Control of robot manipulator with bounded disturbances. *Robust Control with Engineering Applications*. 535437.

[22] Armstrong B and Wade BA (2016) Nonlinear PID control with partial state knowledge: Damping without derivatives. *International Journal of Robotics Research*. 19(8).

[23] Daniel Abebe Beyene (2024) *Modern Control System Lecture Note*. Addis Ababa Science and Technology University.

[24] Wang T, Wang H, Wang C and Hu H (2022) A novel PID controller for BLDCM speed control using dual fuzzy logic systems with HSA optimization. *Scientific Reports*. 12, 11316.

Contribution of Individual Authors to the Creation of a Scientific Article (Ghostwriting Policy)

The authors equally contributed in the present research, at all stages from the formulation of the problem to the final findings and solution.

Sources of Funding for Research Presented in a Scientific Article or Scientific Article Itself

No funding was received for conducting this study.

Conflict of Interest

The authors have no conflicts of interest to declare that are relevant to the content of this article.